Accepted Manuscript

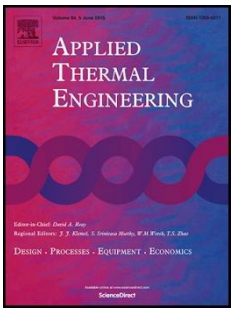

Title: Thermal performance of a new CPC solar air collector with flat micro-heat pipe arrays

Author: Ting-ting Zhu, Yan-hua Diao, Yao-hua Zhao, Feng-Fei Li

PII: S1359-4311(16)00088-0
DOI: http://dx.doi.org/doi: 10.1016/j.applthermaleng.2016.01.033
Reference: ATE 7593

To appear in: *Applied Thermal Engineering*

Received date: 30-7-2015
Accepted date: 8-1-2016

Please cite this article as: Ting-ting Zhu, Yan-hua Diao, Yao-hua Zhao, Feng-Fei Li, Thermal performance of a new CPC solar air collector with flat micro-heat pipe arrays, *Applied Thermal Engineering* (2016), http://dx.doi.org/doi: 10.1016/j.applthermaleng.2016.01.033.

Thermal performance of a new CPC solar air collector with flat micro-heat pipe arrays

Ting-ting Zhu, Yan-hua Diao*, Yao-hua Zhao, Feng-Fei Li

The Department of Building Environment and Facility Engineering, The College of Architecture and Civil Engineering, Beijing University of Technology, No.100 Pingleyuan, Chaoyang District, Beijing 100124, China

Highlights

- A new type of CPC solar air collector with flat micro-heat pipe arrays is proposed.
- The instantaneous efficiency of the collector can reach 62% during the test period.
- The pressure drop is less than 36.8 Pa. The friction factor was also determined.

Abstract

A new type of compound parabolic concentrator (CPC) solar air collector (SAC) with flat micro-heat pipe arrays (FMHPA) was investigated in this study. A cylindrical absorber was constructed by inserting the FMHPA into an evacuated glass tube to transport heat during the working process. The new FMHPA-CPC SAC is an edge ray collector with a concentration ratio of 1.8. The core concept is the integration of the FMHPA, an absorber tube, and a CPC reflector as a heat-collecting unit. Thermal performance investigation was conducted theoretically and experimentally. This study mainly analyzed the effect of different factors on the thermal performance

* Corresponding author. Tel.: +86 010 67391608-802; fax: +86 010 67391608-802
E-mail address: diaoyanhua@bjut.edu.cn (Y.H. Diao)

of the collector. The efficiencies and heat loss coefficients of the new collector were determined. Experimental curves with different testing conditions are presented. The optimal value of efficiency was determined for the SAC. The aperture area of each CPC collecting unit is approximately 0.4 m^2. The new FMHPA-CPC SAC was tested in Beijing, China. The average efficiency was approximately 61% at a volume flow rate of 320 m^3/h, with a radiation of 799 W/m^2 (ambient temperature of 28.8 °C). The instantaneous efficiency reached 68%, depending on the solar radiation, air volume flow rate, and ambient temperature. In addition, the time constant of the collector was approximately 14.8 min, with an air volume flow rate of 260 m^3/h.

Keywords: Solar air collector; CPC; Flat micro-heat pipe array; Time constant; Thermal efficiency

Nomenclature

$\dot{m}$	mass flow rate of air, kg/s	l	length of the air duct, m
A_c	daylight area	d_e	hydraulic diameter, m
T_o	average outlet air temperature, °C	g	gravitational acceleration, m/s^2
T_i	inlet air temperature, °C	f	friction factor
c_p	specific heat of air, KJ/kg·K	*Greek*	
Q_u	useful energy gain, W/m^2	α	absorptivity of the absorber film
$\dot{Q}$	volume flow rate, m^3/h	τ	transmittance of transparent cover
T_m	average temperature, °C	ρ	density of air, kg/m^3
T_a	ambient temperature, °C	η_{th}	thermal efficiency
I_T	radiation on tilted surface, W/m^2	*Abbreviatio*	
ΔT	air temperature increase ($T_o - T_i$), °C	FMHPA	flat micro-heat pipe array
ΔP	pressure drop in test length, Pa	CPC	compound parabolic concentrator
ΔI	solar radiation difference, W/m^2	SAC	solar air collector
v	air velocity, m/s	STC	standard test conditions

1. Introduction

Solar collector is a primary component in the heat utilization of solar energy. Flat-plate solar collectors are classified into two broad categories, namely, water and air collectors, based on their heat transfer fluid. Traditional parabolic concentrator collector requires a sophisticated and costly tracking system. Meanwhile, several problems should be considered during application. A compound parabolic concentrator (CPC) collector with special merits has been investigated recently. This collector is mainly composed of a concentrator and a receiver. In the working process of the CPC, solar energy is concentrated on the receiver and absorbed by the body. Subsequently, heat is transmitted to the flow medium in the receiver, which becomes useful energy. Given the advantage of easy operation, several studies have been conducted on the CPC collector.

Oommen [1] designed a CPC solar collector with a 23.5° acceptance half angle, a cylindrical tube receiver, and water as working fluid. The heat-collecting efficiency of the collector is approximately 50%. Zhao [2] analyzed the heat transfer performance of a heat pipe-type vacuum tube CPC collector. Experimental investigation showed that the heat-collecting efficiency of the heat pipe-type vacuum tube CPC collector is higher than those of the heat pipe-type vacuum tube collector and heat pipe CPC collector under the same radiation intensity.

Concentrator design is also an important factor in determining the surface-concentrating characteristics of the collector. Zheng [3] proposed a new type of CPC. The proposed design smoothens the integration point of the involute and parabola, which solves the gap problem of the concentrator and the absorber, and avoids the focus on the reflector to prevent surface damage of the reflector.

A new solar air heater with a conical concentrator, whose absorber was arranged as a two-pass

exchanger and mounted on the focal axis of the conical concentrator, was investigated using several tilting angles and flow rates [4]. The main operation parameters related to the efficiencies of the collector and heat flow were determined, correlated, and compared with those of flat-plate solar collectors.

Türk Toğrul et al. [5] investigated the free convection performance of a solar air heater with a cylindrical absorber centered on a conical concentrator to focus incident solar radiation. With two satellite antenna motors, the system can rotate to ensure that the conical concentrator is continuously facing toward the sun. The efficiencies of the conical solar collector were determined to be similar to those of conventional flat-plate solar collectors. Buttinger et al. [6] developed and investigated a new flat stationary evacuated CPC collector. They reported that heat loss reduction by using thin inert gases is as important as radiation concentration. Thermal test confirmed the theoretical results that collector efficiencies greater than 50% are possible at working temperature of 150 °C at standard conditions.

A solar air heater with a CPC was used in the regeneration of silica gel desiccant [7]. Results show that the optical efficiency and heat loss of the collector are 0.68 and 8.51 W/m^2, respectively. Liu et al. [8] designed a novel evacuated tubular solar air collector (SAC) integrated with a simplified CPC and special open thermosiphon. They used water-based CuO nanofluid as working fluid to provide air with high and moderate temperatures. The maximum air outlet temperature exceeds 170 °C at an air volume rate of 7.6 m^3/h in winter.

A method (Chungpaibulpatana and Exell) for measuring the performance parameters of a solar thermal collector is used to analyze the performance of a solar flat-plate collector with a CPC for heating air instead of water. The method can be applied to an air heater with a truncated CPC under

nonsteady-state conditions [9]. In addition, numerical investigations have been conducted in recent years [10,11]. A mathematical model of the optical and thermal performance of non-evacuated CPC solar collectors with a cylindrical absorber was described [12]. The results show that heat loss coefficients are accurately represented by a second-degree polynomial in ΔT_a. Kim et al. [13] investigated numerically and experimentally the performance of an evacuated CPC solar collector with a cylindrical absorber and an internal reflector . Two types of evacuated CPC (stationary and tracking) solar collectors are designed, manufactured, and tested under outdoor field conditions. The result shows that the thermal efficiency of the tracking CPC solar collector is more stable and approximately 14.9% higher than that of the stationary CPC solar collector.

Due to the high energy storage density and the isothermal nature of the heat storage, phase change material (PCM) energy storage is advantageous in certain applications for the solar air collectors. A solar air collector with a paraffin type phase change material (PCM) energy storage subsystem was investigated by Enibe [14]. And the day-long maximum predicted cumulative useful and overall efficiencies are 13% and 18%, respectively. S. Bouadila et al. [15] conducted an experimental investigation to evaluate the thermal performance of a solar air heater collector using a packed bed of spherical capsules with a latent heat storage system, which can stored solar energy in the packed bed through the diurnal period and extracted at night. Energy and exergy analysis of the solar air heater with latent storage energy have been done in 2014 by S. Bouadila et al. [16]. When a solar air collector was used to support the heating of building, latent heat thermal energy storage (LHTES) is necessary during the period of night. A solar air heating system with LHTES was developed by Arkar and Medved [17].

To the best of our knowledge, studies on the thermal performance of the CPC SAC with heat pipes

are rarely reported. Only a few studies [7,8,18] have conducted investigations on the thermal performance of the CPC SAC. In this paper, a new kind of solar air heater-the flat micro-heat pipe array CPC solar air collector (FMHPA-CPC SAC) is presented. The heat transfer and flow friction characteristics for FMHPA-CPC SAC were also investigated.

2. Collector detail and experimental system

2.1. Flat micro-heat pipe arrays

FMHPA technology [19,20] is a new type of heat transfer system with advantages of high heat transfer ability, high reliability, and low cost. The FMHPA has been gradually applied to solar heat, heat dissipation of electronic devices, and other various heat fields. The shape of FMHPA is shown as Fig. 1, which is similar to that of a thin aluminum plate, wherein more than 10 independent micro heat pipes exist inside each FMHPA, and the micro-fin structure in each micro heat pipe can significantly improve the heat exchange area. It is formed by multiple micro heat pipes together, which is simultaneous completely independent with each other, and each micro heat pipe is not connected through. In each micro-channel heat pipe, there contains many miniature axially grooves or micro-fins inner to enhance the heat transfer. Each FMHPA can be divided into two sections: evaporator section and condenser section. The operation principle of the FMHPA is shown as Fig.2. When the evaporator section is heated, the working fluid filling in the evaporator section evaporates to saturated vapor, and then the vapor flows upward to the condenser section under pressure difference. In the condenser section, the vapor condenses to liquid and releasing heat, and then the condensing liquid returns to the evaporator section by gravity and capillary force. The phase change cycle achieve the heat transmission from evaporator section to the condenser section.

The FMHPA is manufactured by extrusion process with aluminium profile completely, and then

filling working medium inside the extrusion through-hole to forming the micro heat pipe by vacuumize operation using vacuum pump, and form FMHPA with encapsulation eventually. The vacuum degree of FMHPA is kept at 10^{-4} Pa. The length can be determined according to the demand of the specific application conditions. The FMHPA can fit well with heat exchange surface, and its heat transport capability is strong.

A basic test was conducted to show the thermal performance of the FMHPA used in the new collector. The dimension of the FMHPA in the present study is 1,800 × 40 × 3 mm^3.The test system and the test results are shown in Fig. 3. In the testing process, the evaporator section was inserted into a thermostatic water bath, and the working conditions were maintained at 60, 70 and 90 °C, respectively. The condenser section was cooled by natural convection in the indoor environment (indoor temperature is 20 °C). A total of 5 T-type thermocouples were installed along the condenser section of FMHPA with a space of 400 mm. Agilent 34970A was used to record the testing data. Fig. 3 shows that the response time of the FMHPA is less than 180 s in different testing conditions. The results revealed that FMHPA has a high thermal respond speed. Therefore, the FMHPA exhibits excellent heat transfer performance and can serve as a dominant component of the new SAC.

The new air collector with a built-in micro-heat pipe array in vacuum tube has a cylindrical absorber, reflector half angle of 30°, and concentration ratio (CR) of 1.8. The FMHPA, as the core technology of the CPC collector, is a breakthrough and innovation. The heat gained by the receiver increases because of better effect of the reflector. However, heat loss also increases mainly because the temperature of the absorber glass is higher than that of the outlet air temperature, which causes radiation emission from the selective absorbing film surface to increase, as expressed in the Stefan–Boltzmann law. The vacuum glass tube can minimize convective heat loss. The vacuum layer

of the space between the outer glass tube and absorbing tube can partly overcome this problem.

2.2. Structure of the novel FMHPA-CPC SAC

FMHPA-CPC SAC comprises an air collector body, air duct, and fan (Fig. 4). The air collector body is composed of 10 new CPC heat-collecting units. Each unit comprises FMHPA, an evacuated glass tube, fins, and a CPC reflector. The parameters of each component are shown in Table 1. Each heat collecting unit is composed of CPC, vacuum tube and FMHPA heat transfer unit. One section (condenser section) of each FMHPA is embedded in the gap of two back-to-back fins by mechanical means as heat transfer unit; the other section of the FMHPA (evaporator section) is inserted in the vacuum tube. The section with fins is placed in the interior of the air duct shown as Fig.5.

2.2.1. Composition of the collecting unit

The receiver of the FMHPA-CPC SAC is cylindrical, and the FMHPA is inserted into the evacuated glass tube. Fig. 6 shows the schematic of the CPC collecting unit and cylinder receiver. Solar radiation energy is absorbed by selective absorbing coating of the evacuated glass tube. The heat is then transferred to the site with fins by the FMHPA (heat is transferred from the evaporator to the condenser section of the FMHPA via phase change heat transfer process), and heat exchange occurs between high-temperature fins and cool air that flows through the fins. The cool air is warmed during the heat transfer process.

2.2.2. CPC structure

The cross-section of FMHPA-CPC SAC exhibits axial symmetry around the *Y*-axis symmetric design of the condensing surface, with the right branch composed of a section of the parabola and a section of the circle involute, which are connected by a curve. In the experiment, the outer and inner diameter of the vacuum glass tube was 58 and 47 mm, respectively. To avoid errors in manufacturing

and assembling processes, the radius of the inner tube used in the equation can be smaller than the actual value [21]. So, using 23 mm as the radius value of the equation, and the curve equation of CPC cross-section in the present study can be written as follows:

involute equation:

$$\begin{cases} x = 23\sin\theta - 23\theta\cos\theta \\ y = -23\cos\theta - 23\theta\sin\theta \end{cases} \qquad 0 \le \theta \le \frac{\pi}{2} + \frac{\pi}{6}, \quad (1)$$

parabolic equation:

$$\begin{cases} x = 23(\sin\theta - \dfrac{\pi/2 + \pi/6 + \theta - \cos(\theta - \pi/6)}{1 + \sin(\theta - \pi/6)}\cos\theta) \\ y = -23(\cos\theta - \dfrac{\pi/2 + \pi/6 + \theta - \cos(\theta - \pi/6)}{1 + \sin(\theta - \pi/6)}\sin\theta) \end{cases} \qquad \frac{\pi}{2} + \frac{\pi}{6} \le \theta \le \frac{3\pi}{2} - \frac{\pi}{6}. \quad (2)$$

In the previously presented formulas, θ denotes the angle between the incident ray and *X*-axis parallel lines.

In this study, the condenser surface is composed of a highly reflective stainless steel plate molding, with a geometric CR of 2. Considering economic factors in practical application, the original design of the CPC condenser is truncated by 43.6% based on a CR of 1.8. The concentrator plate thickness is 1.0 mm, plate reflectivity is 0.92, actual height of CPC is 186.5 mm, length is 1.5 m, and notch area is 0.268 × 1.5 = 0.40. The condenser structure and section size are shown in Fig. 7.

2.2.3. Working process of the collector

FMHPA is a high-efficiency heat transfer component, which is dependent on the phase change of the working fluid filling the micro-channels of the FMHPA. During the working process, each FMHPA has two parts, namely, the condenser and evaporator sections. The lengths of the evaporator and condenser sections are 1,620 and 180 mm, respectively. As shown in Fig. 8, the FMHPA is a flat aluminum plate with several independent micro-channels. Each micro-channel can be considered as

an independent heat pipe.

The evaporator section is inserted into the vacuum tube, and the condenser section is attached to the aluminum fins [22]. The basic working principle of the new type of FMHPA-CPC SAC is that some of the incident solar radiation is directly absorbed by the outer layer of the vacuum glass and subsequently absorbed by the inner layer with selective absorbing coating. The rest of the solar radiation absorbed by the surface of the CPC reflector is subsequently reflected to the vacuum tube through one or two reflections. Thus, almost all the solar radiation obtained by the collector has been absorbed by the vacuum tubes. Heat is then transferred to the evaporator section of the FMHPA. The working fluid (acetone, with 20% liquid filling ratio) in the evaporator section absorbs the heat and begins to evaporate. The vapor flows up to the condenser section. In this section, the vapor condenses to liquid after energy is released through the fins and returns to the evaporator section by gravity and capillary force. In general, heat is transmitted to the fins (condenser section) via phase change through the FMHPA during this process. Finally, the air is heated when it flows through the fins. The FMHPA is a high-efficiency heat transfer element for the solar thermal field. Solar radiation exists transiently; thus, using FMHPA can improve the output energy of the collector. Meanwhile, the thermal diode effect of the FMHPA can reduce the heat transferred to the surrounding environment when solar radiation is low.

2.3. Experiments

2.3.1. Test facility

The experimental setup of the FMHPA-CPC SAC is installed outdoors at Beijing University of Technology (39.92 N, 116.43 E), as shown in Fig. 9. The tilt of the collectors with respect to the horizontal plane is 45° toward south. Performance tests of the new collector were conducted under

clear sky.

The following variables were measured for each test:

(i) Inlet and outlet air temperatures.

(ii) Temperature at different testing points on the surface of FMHPA and fins;

Temperatures on the surface of the vacuum inner wall;

Air temperature inside the vacuum tube.

(iii) Air velocity.

(iv) Ambient temperature.

(v) Wind velocity and wind direction.

(vi) Global solar irradiation incident on the collector plane.

(vii) Pressure drop across the collector.

The FMHPA and fins of the collector were fitted with T-type thermocouples for measuring temperatures at different testing points. The air duct was fitted with PT100-type thermoresistances at each cross-section of the inlet and outlet. The inlet and outlet air flow temperatures were measured by four thermoresistances (Fig. 10). The experimental setup was adjacent to the weather station that measured the ambient temperature, wind velocity and direction, and global solar irradiation. A TRT-2 pyranometer was used to measure global solar irradiation in the plane of the FMHPA-CPC collector during the day. A Testo512 differential manometer was used to measure the pressure drop across the collector. The air flow rate was tested using air volume cover. Information and uncertainties about the test instruments are shown in Table 2.

Error estimation of thermal efficiency depends mostly on the thermoresistance errors at eight points and the accuracy value of the other parameters. Considering the relative errors of the

individual factors denoted by x_n, the relative error of efficiency was calculated using the following equation [23] and was determined to have been changed by ±4.53% to ±4.95%:

$$W = [(x_1)^2 + (x_2)^2 + \cdots + (x_n)^2]^{1/2}. \quad (3)$$

2.3.2. Test procedure

Tests were conducted for approximately half a year, from June 4 to December 22, 2014. All meteorological parameters were recorded by an automatic recording apparatus connected to a meteorological station with 1 min time interval. The other temperature parameters were recorded by the data acquisition system (Agilent 34970A) with a preset time interval. For each test condition, the air flow rate was not changed once the test began. Four operational modes were investigated by setting different flow rates. In each calculation, the average temperature of the evaporator section was used. Moreover, the evaporator section was considered the constant temperature section. Collector performance was monitored by measuring air duct flow rate and temperature, solar irradiance, and testing point temperature.

Instantaneous thermal performance is an important parameter used to evaluate the performance of the collector system. Notably, all data in the experiment were recorded instantaneously with a certain stable air mass flow rate, but transient solar radiation intensities. The performance of the collector varies continuously because solar radiation changes with time during the day. As such, when the instantaneous experiment begins, part of the solar energy absorbed by the vacuum tube is used to heat up the components of the collector.

In addition, time constant can be used to determine the response time of the SAC to evaluate the transient behavior of the collector. Time constant is defined as the time required for the fluid leaving a solar heater to attain 63.2% of its steady-state value following a steep change in irradiation or inlet

fluid temperature. Time constant is the time required for the quantity $(T_{o,t} - T_i)/(T_{o,i} - T_i)$ to change from 1.0 to 0.368, where $T_{o,t}$ is the temperature of the air leaving the collector at a specified time, $T_{o,i}$ is the temperature of the air leaving the collector at the beginning of the specified time period, and T_i is the temperature of the air entering the collector [24].

3. Analysis

3.1. Optical efficiency of the collector

The optical efficiency of the CPC is defined as follows [1]:

$$\eta_O = \rho_m^n \tau_e \alpha_r p f_{ref}, \quad (4)$$

where τ_e is the transmittance of the vacuum glass tube; α_r is the absorbance of selective coating film; ρ_m is the reflectance of the material of the reflector of the CPC, $\rho_m^n = \rho_m^{(1+0.07CR)}$; p is the loss coefficient of the gap, $p = 1 - g/2\pi r_1$, where g is the gap thickness and r_1 is the radius of the absorber; f_{ref} accounts for the multiple reflections between the absorber tube and the glass tube, $f_{ref} = \left[1 - \rho_r \rho_e (A_r / A_e)\right]^{-1}$; ρ_r is the reflectance of the vacuum glass tube, $\rho_r = 1 - \alpha_r$; and ρ_e is the reflectance of the outer tube of the vacuum glass tube. The parameters of the reflector are shown in Table 3.

The calculated value of the optical efficiency of the FMHPA-CPC SAC is 0.656.

3.2. Heat transfer resistance between different components

Assuming that there is good contact between the fins and the FMHPA, and considers the FMHPA as high efficient heat transfer component. Thus, the internal heat transfer resistance between the different components of the collector is calculated as follows,

(1) Thermal conduction resistance between the fins and MHPA at the condenser section:

$$R_1 = \frac{\delta}{\lambda \cdot A} = \frac{\delta}{\lambda \cdot w \cdot l}$$
$$R_1 = \frac{1.0 \times 10^{-3}}{3.0 \times 0.04 \times 0.1} = 0.083\ \mathrm{K/W}. \quad (5)$$

(2) Thermal convection resistance between fins and air in the duct:

$$R_2 = \frac{1}{h \cdot A} = \frac{1}{h \times 0.016}$$
$$R_2 = \frac{1}{(5.7 + 3.8 \times 2.08) \times 0.016} = 4.594\ \mathrm{K/W}. \quad (6)$$

(3) Thermal resistance of the air duct insulation board:

Thermal resistance of heat conduction of the insulation board:

$$R_3 = \frac{\delta}{\lambda} = \frac{0.025\ \mathrm{m}}{0.024\ \mathrm{W/m \cdot k}} = 1.04\ \mathrm{m^2 \cdot K/W}, \quad (7)$$

Thermal resistance of heat convection between the insulation plate and air:

$$R_4 = \frac{1}{h} = \frac{1}{5.7 + 3.8 \times 3} = 0.0585\ \mathrm{m^2 \cdot K/W}. \quad (8)$$

4. Results and discussion

4.1. Determination of the time constant of the collector

In general, the components of the collector mainly comprise several heat-collecting units and air ducts, which results in thermal inertia of the heat collector. The time constant can reflect the level of thermal inertia of the collector. Hou et al. [25] proposed a modified method to test the time constant based on the method provided in Ref. [24]. The modified method defined time constant as the time required for the quantity of $\left(T_{f,o}(\tau) - T_{f,o,initial}\right) \Big/ \left(T_{f,o,\infty} - T_{f,o,initial}\right)$ to change from 0 to 0.632, where $T_{f,o}(\tau)$ is the outlet temperature of the air collector at a specified time, $T_{f,o,\infty}$ is the outlet temperature at the end of the specified time period, and $T_{f,o,initial}$ is the outlet temperature of the heater at the beginning of the specified time period. Using this method needn't to adjust the inlet temperature of the collector equals to the ambient air temperature, which has been verified by the

experimental results.

In the present study, we used the method of Hou et al. [25] to determine the time constant of the FMHPA-CPC SAC. The air velocity was 3.0 m/s at the entrance when the collector time constant was approximately 14 min. Fig. 11 shows the curve of the time constant. The working fluid of the collector is air, and the heat capacity of air is small. As such, the solar radiation was reduced and the effect of thermal inertia is evident in the initial period. Conversely, the efficiency increased at this moment.

4.2. Thermal efficiency

The heat collection efficiency of the SAC is the ratio of useful energy and actual solar energy absorbed, which is one of the most important parameters of solar collector performance. Efficiency can be defined as follows [4]:

$$\eta = \frac{Q_u}{A_c I_t}, \qquad (9)$$

During the experimental process, the instantaneous thermal efficiency of the collector is obtained by using the following formula:

$$\eta = \frac{c_p \dot{m} (T_o - T_i)}{A_c I_t}, \qquad (10)$$

A detailed set of experiments was conducted under clear weather. The collector was operated in the open loop mode to investigate its performance at different operating conditions. Fig. 12 shows the weather condition on June 7, 2014. The air volume flow rate was 320 m^3/h under this testing condition. During the test period (9:00 AM to 3:30 PM), the solar radiation was between 513 and 936 W/m^2 with only a slight fluctuation and the environmental temperature fluctuated between 24.9 and 32.7 °C. The relative humidity values were between 30.5% and 46.9%, and wind speed fluctuated between 0.2 and 2.1 m/s.

The variation of outlet temperature and efficiency with the set flow rates for the FMHPA-CPC SAC is shown in Fig. 13. The outlet temperature of the collector was between 26.3 and 51.1 °C. The instantaneous thermal efficiency reached approximately 67.7% during the test period. Thermal efficiency and outlet temperature evidently increased before 10:42 AM, which reveals that thermal efficiency increased with increasing solar radiation intensity. After 10:42 AM, the outlet temperature slightly increased and the thermal efficiency varied between 50% and 67.7%. After 2:00 PM, the thermal efficiency decreased sharply because of the decreased incident solar radiation of the CPC plate. The results reveal that the efficiency enhances as the solar radiation intensity, and outlet temperature of the FMHPA-CPC SAC are strongly dependent on solar radiation when the air flow maintain at a constant value.

Fig. 13 shows that the receiver and reflector absorbed the solar radiation completely beginning at 10:00 AM. Solar thermal efficiency increased with increasing average intensity of solar radiation. The average efficiency of the collector was approximately 53%. Fig. 14 shows the temperature behavior of the FMHPA, inlet temperature, and outlet temperature during this period. The difference between the evaporator section temperature T_e and condenser section temperature T_c reached 20 °C when the solar radiation is more than 600 W/m^2. At the same time, the fluctuation of the solar radiation value influence the temperature distribution of the FMHPA as well as the outlet temperature. When the solar radiation decreased, the temperatures of the evaporator and condenser sections of the FMHPA decreased immediately. The fluctuation point occurs at the time that solar radiation fluctuated. The findings showed that solar radiation plays an important role as the heat source of the collector, which can determine the input quantity of heat collected by the collector directly.

Fig. 15 illustrates the arrangement of thermocouples on the FMHPA and fins. In this study, the

FMHPA used in the collector was 1.8 m long. Fig. 16 shows the variation of different temperatures on the FMHPA during the testing period (four days). The temperature values of T1 and T2 are close, but T2 is slightly higher, which showed the superior temperature uniformity of the FMHPA. The difference between T2 and T1 was approximately 4 °C. The temperature value of T3 represents the condenser section temperature of the FMHPA, which is approximately 17 °C lower than that of the evaporator section temperature. The temperature difference between the condenser and evaporator sections is mainly attributed to forced convection heat transfer.

Fig. 16 shows that the evaporator and condenser section temperatures of the FMHPA reached 126.2 and 115.8 °C, respectively, on June 7, 2014. With the increase in the intensity of solar radiation and ambient temperature at 10:00 AM, the collector outlet air temperature increased. By contrast, with the decrease in the solar radiation intensity at 2:00 PM, the incident light absorbed by the CPC decreased. As such, the vacuum tube temperature, evaporator and condenser section temperatures, and outlet temperature decreased. By contrast, with the decrease in the solar radiation intensity at 2:00 PM, the incident light absorbed by the CPC decreased. As such, the vacuum tube temperature, evaporator and condenser section temperatures, and outlet temperature decreased.

Table 4 shows the experimental results of certain days in June. These testing conditions included two air flow rates of 320 and 260 m^3/h and their corresponding Reynolds numbers ($\mathrm{Re} = \rho Qd / \mu$) of 37,500 and 30,405, respectively, based on the present collector characteristic length. The flows encountered turbulent flow regimes, which indicate that the Reynolds number increases with increasing air volume flow rate. A high Reynolds number usually results in high heat transfer coefficients and high efficiencies. A high thermal efficiency with low heat losses was also observed. With similar weather conditions, the FMHPA-CPC SAC showed discrepant thermal performance.

Fig. 17 shows the comparison result between two working conditions with different air volume flow rates. Two sets of experiment were conducted on August 25 and 26 under clear and fine weather. The efficiency increased with increasing solar radiation. However, the efficiency decreased at noon because of the increased heat loss of the SAC. Fig. 17 shows the effect of air velocity on the thermal efficiency of the new FMHPA-CPC SAC. With almost the same weather conditions, two different thermal properties were achieved, which were caused by different convection heat transfer conditions. Compared with the experimental result on August 26 with the air volume flow rate of 260 m^3/h, the efficiency on August 25 with the air volume flow rate of 320 m^3/h was higher. A high Reynolds number usually results in high heat transfer coefficients and high efficiencies. These findings indicate that heat transfer enhancement can be achieved with a high volume flow rate.

Fig. 18 shows a part of the experimental results in December. Four different days were used to show the properties of the new FMHPA-CPC SAC. Fig. 18 shows the effect of the weather situation and operating parameters on thermal efficiency. Under the given operating conditions, the solar radiation, air volume flow rate, and weather condition were comprehensive influencing factors of the thermal properties of the collector.

The thermal performance of the collector can be represented by the curve of efficiency versus the reduced temperature parameters $(T_i - T_a)/I$ (Fig. 19). These data were obtained using four different inlet temperatures (28.5, 33.5, 36.5, and 42.5 °C). During the experimental process, we controlled the inlet temperature by using a fin–tube heat exchanger connected to a constant temperature water bath. As shown in Fig. 19, the efficiency curve decreased with increasing temperature parameters. The linear relationship between η and $(T_i - T_a)/I$ is determined as follows:

$$\eta = 0.644 - 8.22\left(\frac{T_i - T_a}{I}\right). \quad (11)$$

The experimental value of $F_o(\tau\alpha)$ is 0.644, and the value of the heat loss coefficient F_oU_L is 8.22.

4.3.3. Resistance characteristics of the collector

In the application of the active solar system, the flow resistance of the collector affects the power value of the fan as well as thermal efficiency value of the collector comprehensively. As shown in Fig. 20, the collector resistance characteristic test was conducted in the open loop mode. The pressure drop with different flow rates between inlet and outlet was tested. The fan was installed at the outlet of the air duct. Five flow rates were selected to test the flow resistance of the collector. The test results showed that the flow resistance was less than 36.8 Pa in the 60 m^3/h to 320 m^3/h range. As such, the collector has the advantage of low pressure drop.

The section size of the collector air duct is 200 mm × 120 mm, and the length of the duct is 3,000 mm. The hydraulic diameter of the air duct can be calculated as follows: $d_e = 2WH/(W+H) = 0.15$ m. As such, the pressure drop of the air duct can be expressed as:

$$\Delta P = f \cdot \frac{l}{d} \cdot \frac{\rho v^2}{2}. \quad (12)$$

The values of pressure drop measured for the collector were used to determine the friction factor based on the Darcy–Weisbach equation:

$$f = \Delta P \cdot \frac{d}{l} \cdot \frac{2}{\rho v^2}. \quad (13)$$

The pressure loss values of the air duct under four flow rates (320, 260, 180, and 100 m^3/h) are 36.8, 24.6, 12.1, 4.6, and 2.0 Pa. Friction factor have been plotted as a function of different values of Reynolds numbers ($Re = \rho Q d / \mu$). And the friction factor correlation has been developed for the present air duct with fins of the new collector, which was obtained by the nonlinear curve fitting

based on the experimental data. It can be observed that friction factor decreases with increase in Reynolds number as shown in Fig.21.

5. Conclusions

In this paper, a novel type of CPC-SAC is presented. A series of experiments was conducted in 2014 in Beijing, China to investigate the thermal performance of the novel SAC. The collector exhibited a stable performance during the test period, with an annual average thermal efficiency of 52%. The novel structure effectively improved the heat performance. Based on the experimental investigations, the following conclusions can be drawn:

(1) The unique form of collecting and exchanging heat did not require a circuitous flow of air into and out of the vacuum tube, which resulted in direct heat exchange between air and fins. As such, the power consumption of the fan can be decreased. Thus, the economic efficiency of the new collector was improved.

(2) The theoretical calculation showed that the optical efficiency of the collector is 65.6%. The experimental investigation showed that the instantaneous efficiency of the collector can reach 62% during the test period.

(3) A high Reynolds number usually results in high heat transfer coefficients and high thermal efficiencies. When the air volume flow rate decreased, the thermal efficiency decreased evidently. By contrast, a high thermal efficiency was obtained with low heat loss.

(4) The test results showed that the pressure drop was less than 36.8 Pa in the 60 m^3/h to 320 m^3/h range. The friction factor correlation based on Reynolds number has been developed for the present air duct with fins of the new collector in this study.

Further research is needed to optimize the structure of the fins to improve the heat transfer

conditions of the collector.

Acknowledgments

The project was financially supported by the National Key Technology Research and Development Program of the Ministry of Science and Technology of China (Grant No. 2012BAA13B02) and Scientific Research Project of Beijing Educational Committee (Grant No. 004000546315527). The authors are grateful for their support.

Reference

[1] R. Oommen, S. Jayaraman, Development and performance analysis of compound parabolic solar concentrators with reduced gap losses—oversized reflector, Energy Conversion and Management 42 (2001) 1379-1399.

[2] Y. L. Zhao, H. Zhang, D. D. Zhan, H.T. Yun, Study on thermal efficiency of CPC heat pipe evacuated tubular collectors. Acta Energiae Solaris Sinica, 2007, 28 (9): 1022-1025.

[3] F. Zheng, A.D. Li, A new type of CPC concentrator, Acta energiae solaris sinica 25 (5) (2004) 663-665.

[4] İ. Türk Tŏgrul, D. Pehlivan, The performance of a solar air heater with conical concentrator under forced convection, International Journal of Thermal Sciences 42 (2003) 571–581.

[5] İ.Türk Toğrul, D. Pehlivan, Effect of packing in the airflow passage on the performance of a solar air-heater with conical concentrator, Applied Thermal Engineering 25 (2005) 1349-1362.

[6] F. Buttinger, T. Beikircher, M. Pröll, W. Schölkopf, Development of a new flat stationary evacuated CPC-collector for process heat applications, Solar Energy 84 (2010) 1166–1174.

[7] S. Pramuang, R.H.B. Exell, The regeneration of silica gel desiccant by air from a solar heater with a compound parabolic concentrator, Renewable Energy 32 (2007) 173–182.

[8] Z.H. Liu , R.L. Hu, L. Lu, F. Zhao , H.S. Xiao, Thermal performance of an open thermosyphon using nanofluid for evacuated tubular high temperature air solar collector, Energy Conversion and Management 73 (2013) 135-143.

[9] S. Pramuang, R.H.B. Exell, Transient test of a solar air heater with a compound parabolic concentrator, Renewable Energy 30 (2005) 715–728.

[10] H. Singh, Philip C. Eames, A review of natural convective heat transfer correlations in rectangular cross-section cavities and their potential applications to compound parabolic concentrating (CPC) solar collector cavities, Applied Thermal Engineering 31 (2011) 2186-2196.

[11] Ch. Reichl, F. Hengstberger, Ch. Zauner, Heat transfer mechanisms in a compound parabolic concentrator: Comparison of computational fluid dynamics simulations to particle image velocimetry and local temperature measurements, Solar Energy 97 (2013) 436–446.

[12] N. Fraidenraich, R. De C. F. De Lima, C. Tiba, E. M. De S. Barbosa, Simulation model of a CPC collector with temperature dependent heat loss coefficient, Solar Energy 65 (2) (1999) 99-110.

[13]Y. Kim, G.Y. Han, T. Seo, An evaluation on thermal performance of CPC solar collector, International Communications in Heat and Mass Transfer 35 (2008) 446–457.

[14] S.O. Enibe, Thermal analysis of a natural circulation solar air heater with phase change material energy storage, Renewable Energy 28 (2003) 2269–2299.

[15] S. Bouadila, S.Kooli, M. Lazaar, S. Skouri, A.Farhat, Performance of a new solar air heater with

packed-bed latent storage energy for nocturnal use, Applied Energy 110 (2013) 267-275.

[16] S. Bouadila, M. Lazaar, S. Skouri, S. Kooli, A. Farhat, Energy and exergy analysis of a new solar air heater with latent storage energy, International Journal of Hydrogen Energy 39 (2014) 15266-1527 4.

[17] C. Arkar, S. Medved, Optimization of latent heat storage in solar air heating system with vacuum tube air solar collector, Solar Energy 111 (2015) 10-20.

[18] J. Kasperski, M. Nemś, Investigation of thermo-hydraulic performance of concentrated solar air-heater with internal multiple-fin array, Applied Thermal Engineering 58 (2013) 411-419.

[19] Y. H. Zhao, K. R. Zhang, Y.H. Diao, Heat pipe with micro-pore tubes array and making method thereof and heat exchanging system, P. US NO. 20110203777.

[20] Y. C. Deng, Y. H. Zhao, W. Wang, Z. H. Quan, L. C. Wang, Dan Yu, Experimental investigation of performance for the novel flat plate solar collector with micro-channel heat pipe array (MHPA-FPC), Applied Thermal Engineering 54 (2013) 440-449.

[21] S.Z. Zhang, W.X. Cui, Design Principle of CPC, Solar Energy 5 (2004) 41-43.

[22] T.T. Zhu, Y.H. Diao, Y.H. Zhao, Y.C. Deng, Experimental study on the thermal performance and pressure drop of a solar air collector based on flat micro-heat pipe arrays, Energy Conversion and Management 94 (2015) 447–457.

[23] Gill RS, Singh S, Singh PP, Low cost solar air heater, Energy Conversion and Management 57 (2012) 131-142.

[24] ASHRAE Standard 93-1986. Method of testing to determine the thermal performance of solar collectors. American Society for Heating, Refrigerating and Air-conditioning Engineers, Atlanta (USA), 1986.

[25] H.J. Hou, Z.F. Wang, R.Z. Wang, P.M. Wang, Experimental methods research on solar collector time constant, Acta Energiae Solaris Sinica 27 (2006) 415-418.

[26] A. Kumar, R.P. Saini, J.S. Saini, Experimental investigation on heat transfer and fluid flow characteristics of air flow in a rectangular duct with Multi v-shaped rib with gap roughness on the heated plate, Solar Energy 86 (2012) 1733-1749.

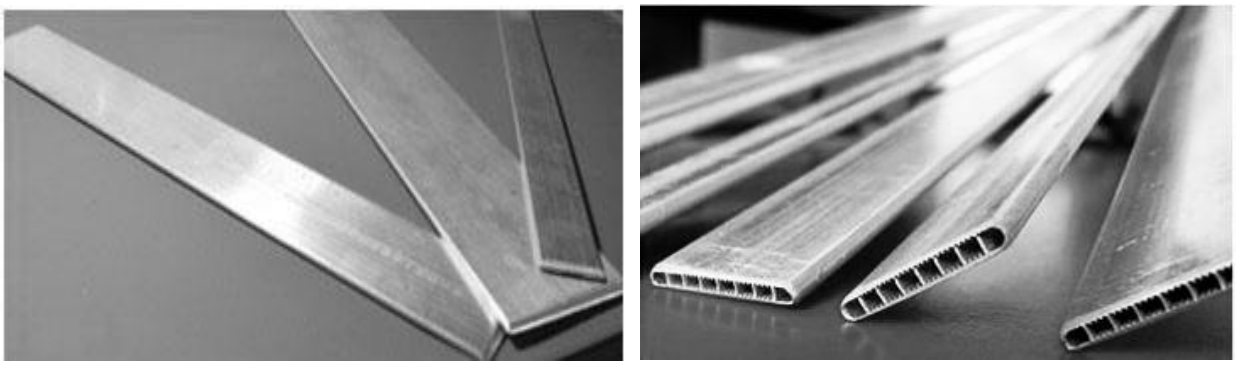

Fig. 1. Pictures of FMHPA.

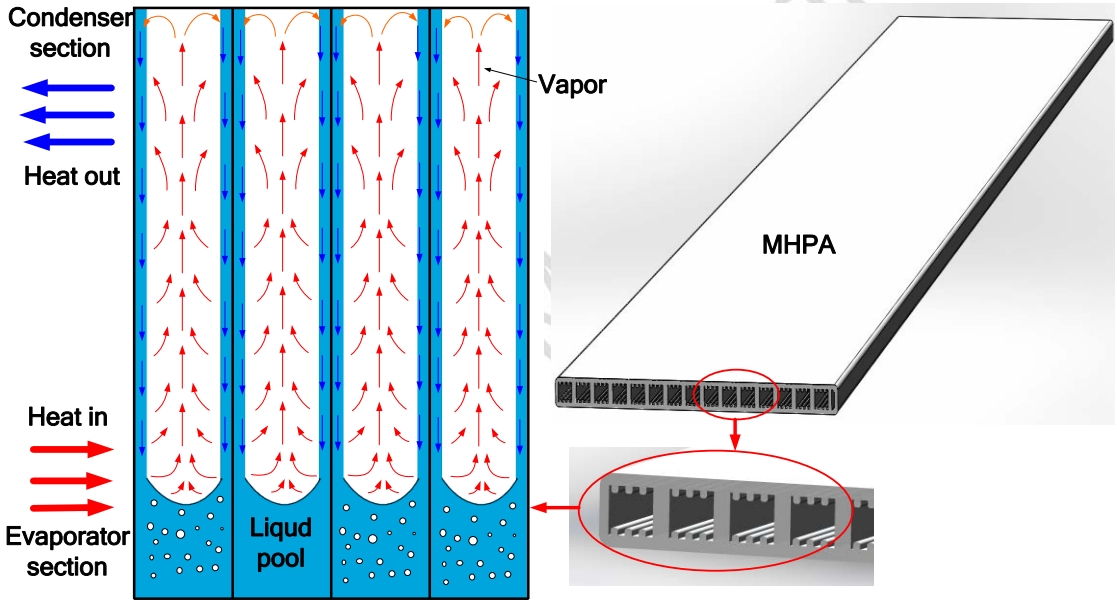

Fig.2. Operation principle of the FMHPA.

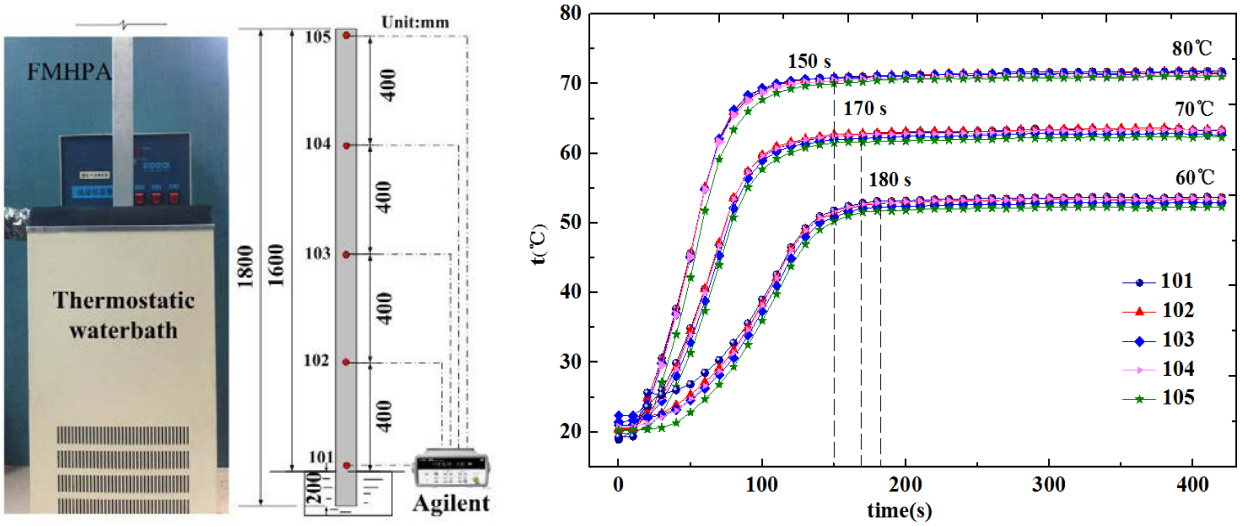

(a) Test system (b) Test results

Fig. 3. Thermal response test of FMHPA.

Fig. 4. Image of the experimental configuration.

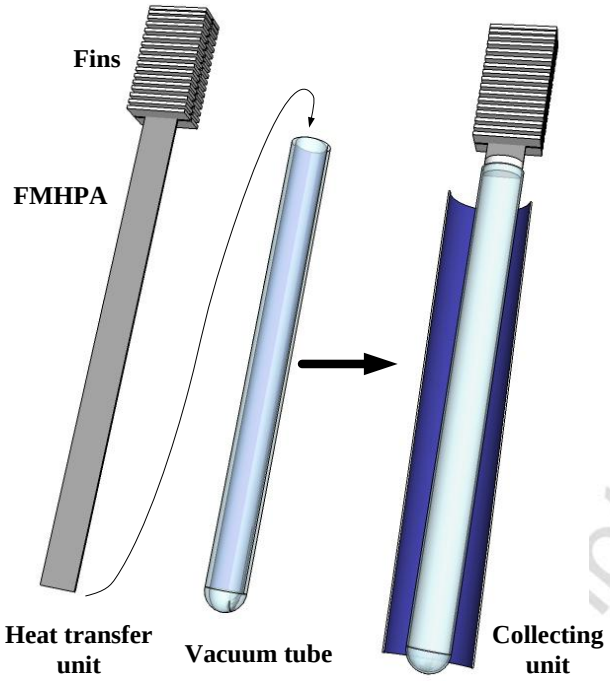

Fig. 5. Diagram of the CPC collecting unit.

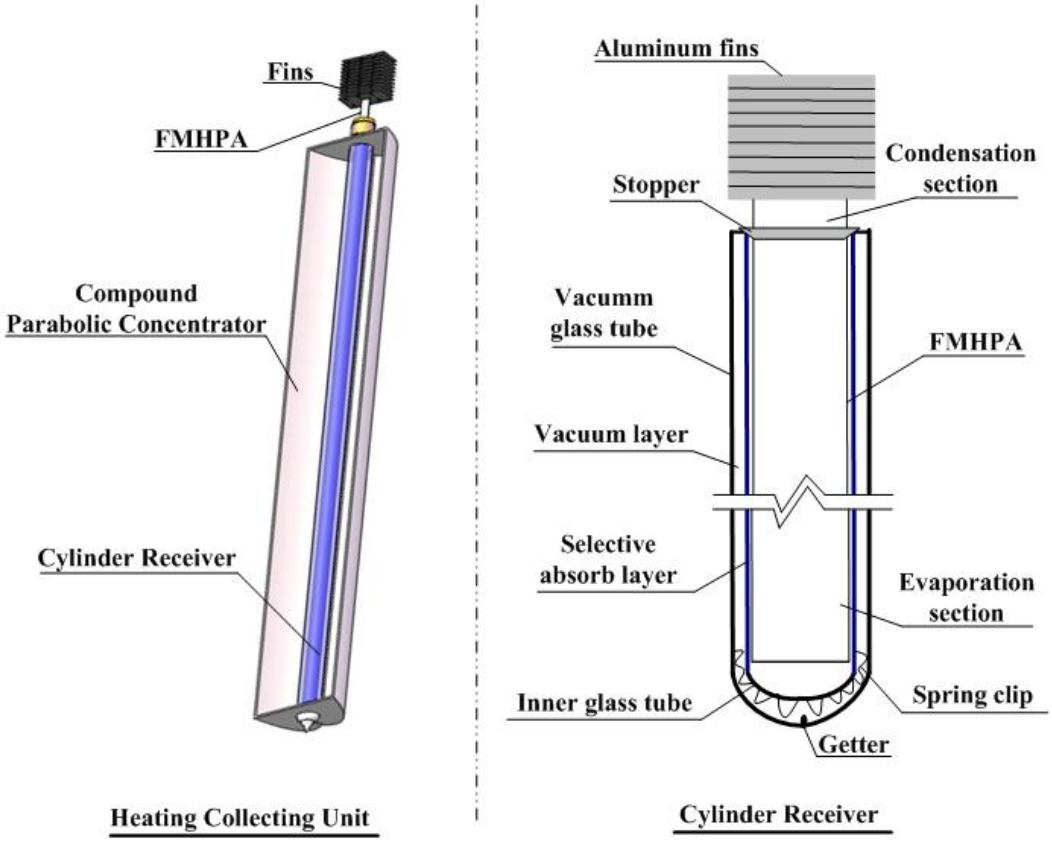

Fig. 6. Schematic of the CPC collecting unit.

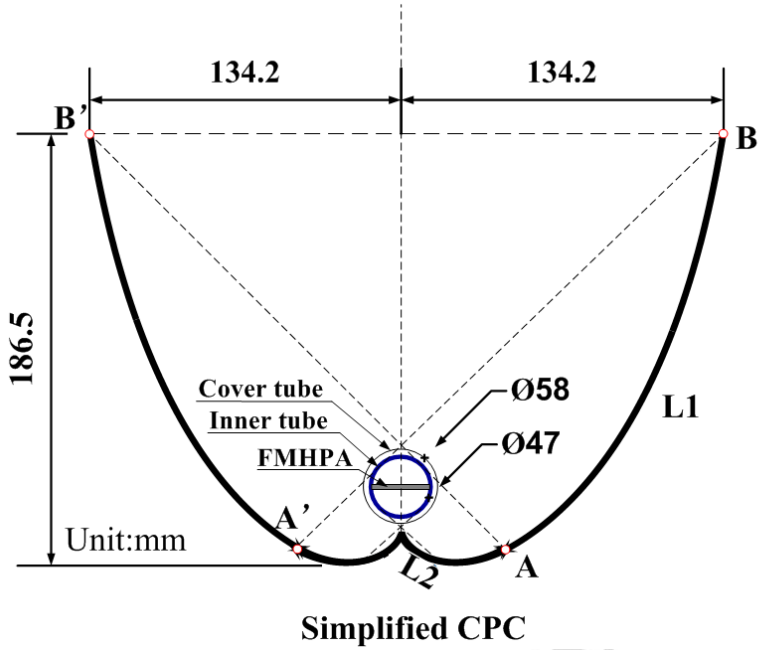

Fig. 7. CPC cross-section diagram.

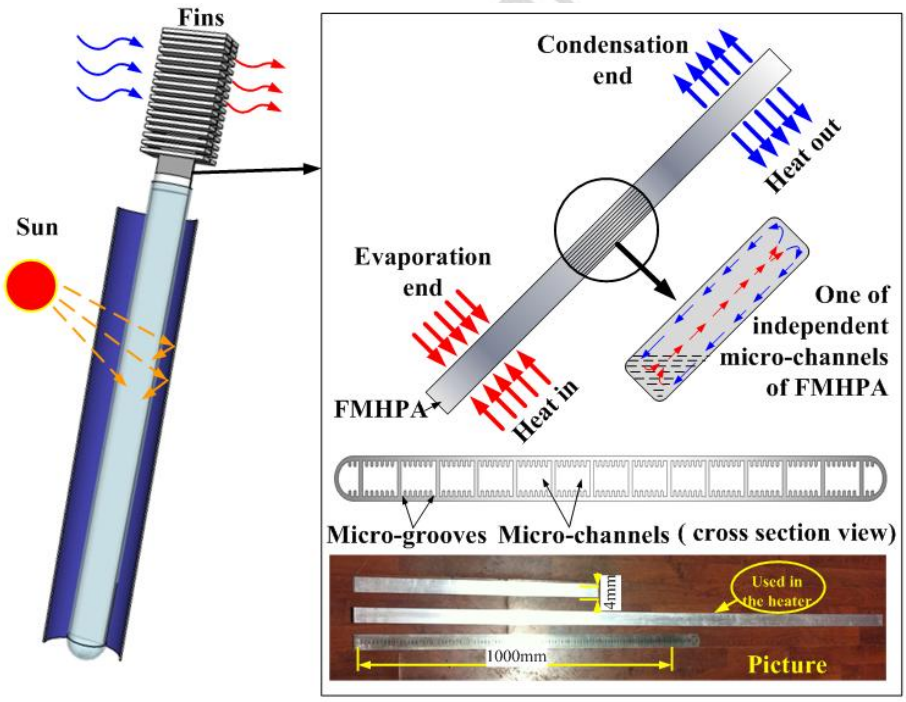

Fig. 8. Heat process and heat-collecting principle diagram.

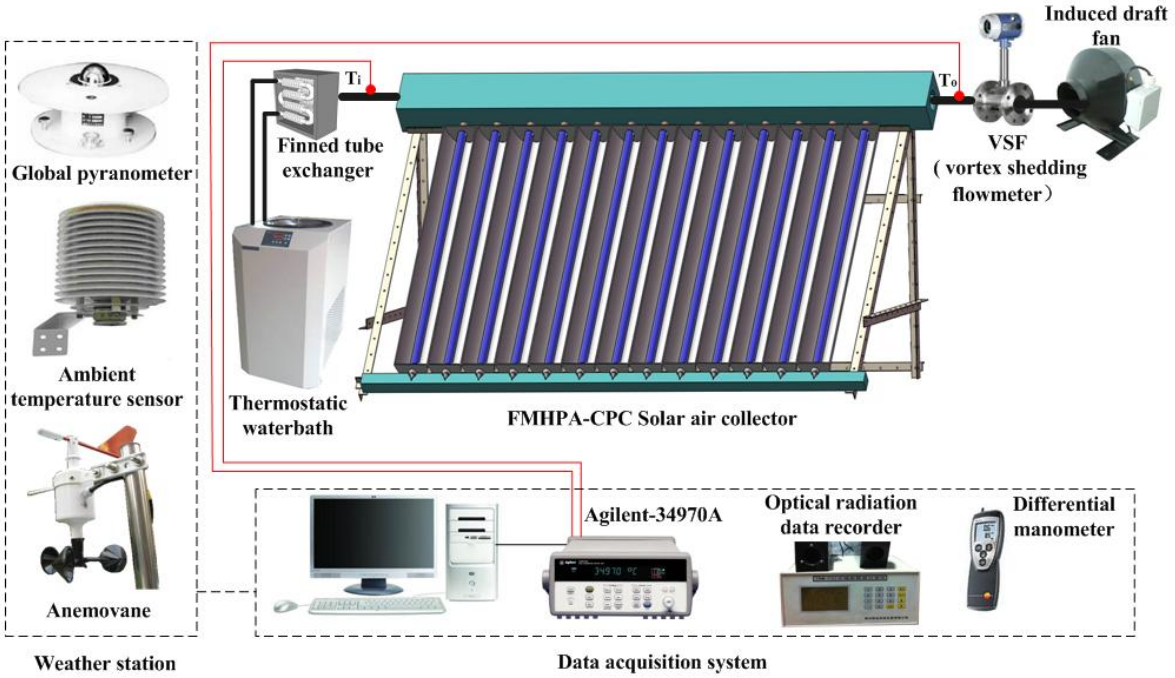

Fig. 9. CPC SAC experimental system.

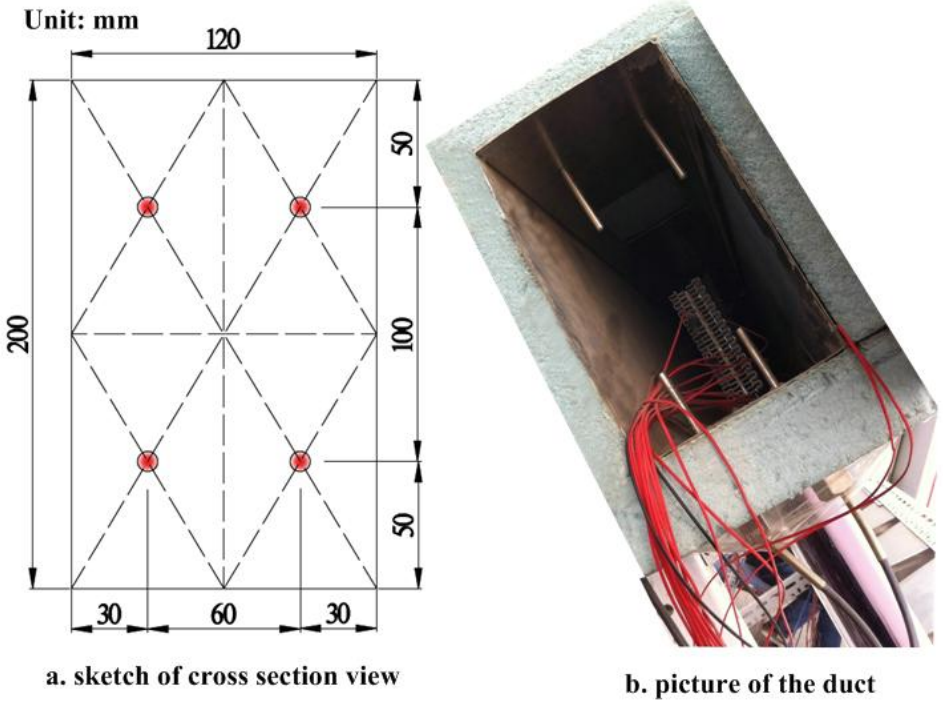

Fig. 10. Arrangement of the measuring points of the inlet and outlet.

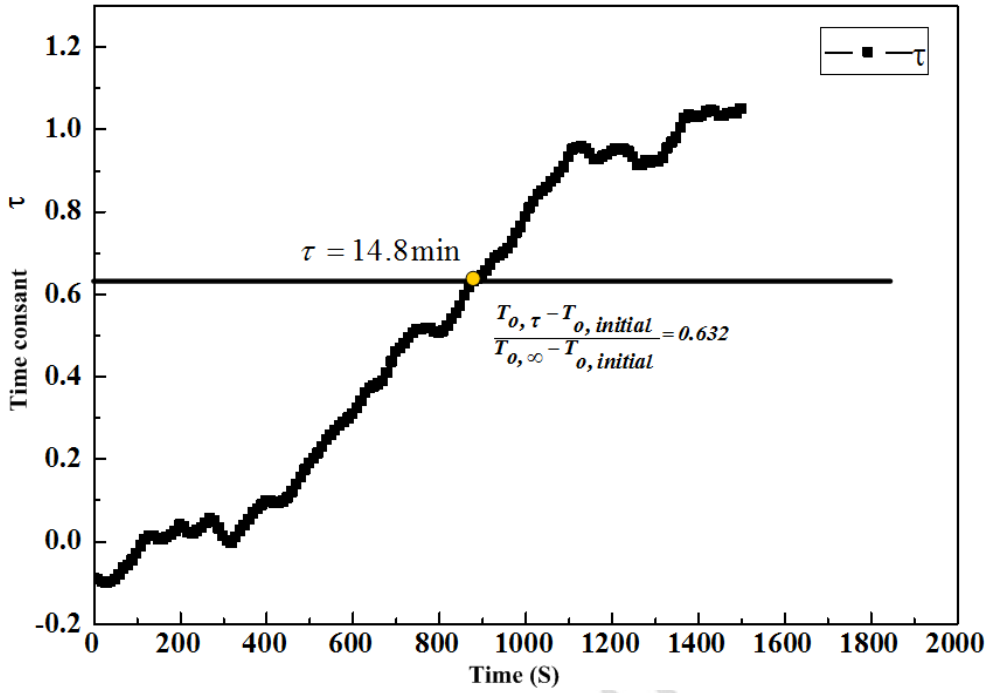

Fig. 11. Time constant curve of the FMHPA-CPC SAC.

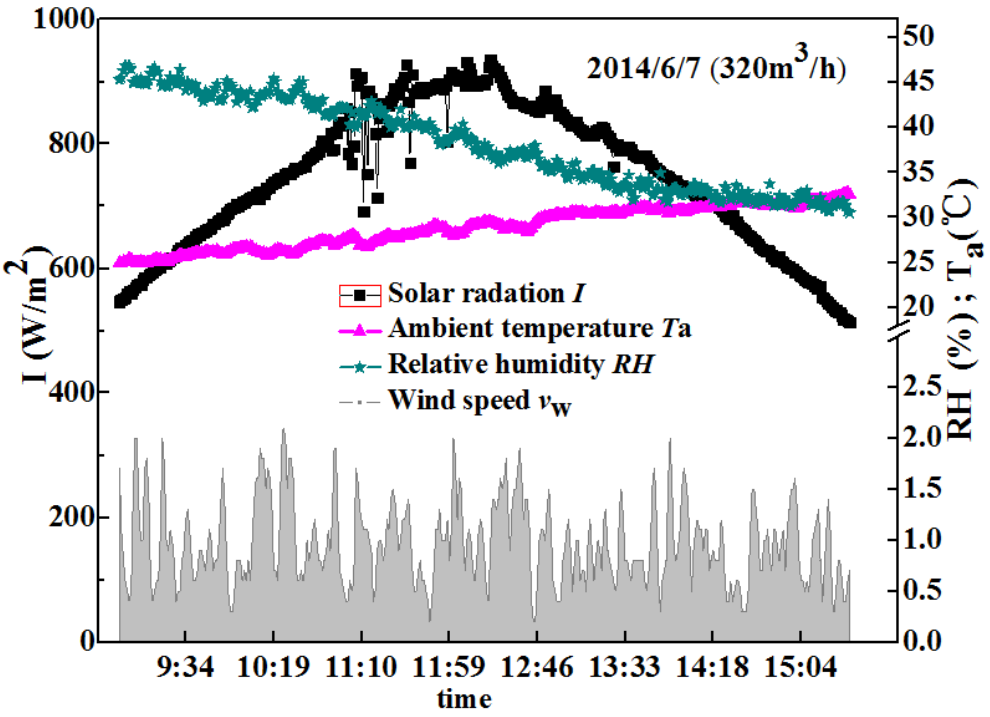

Fig. 12. Variations of meteorological parameters versus time on June 7, 2014.

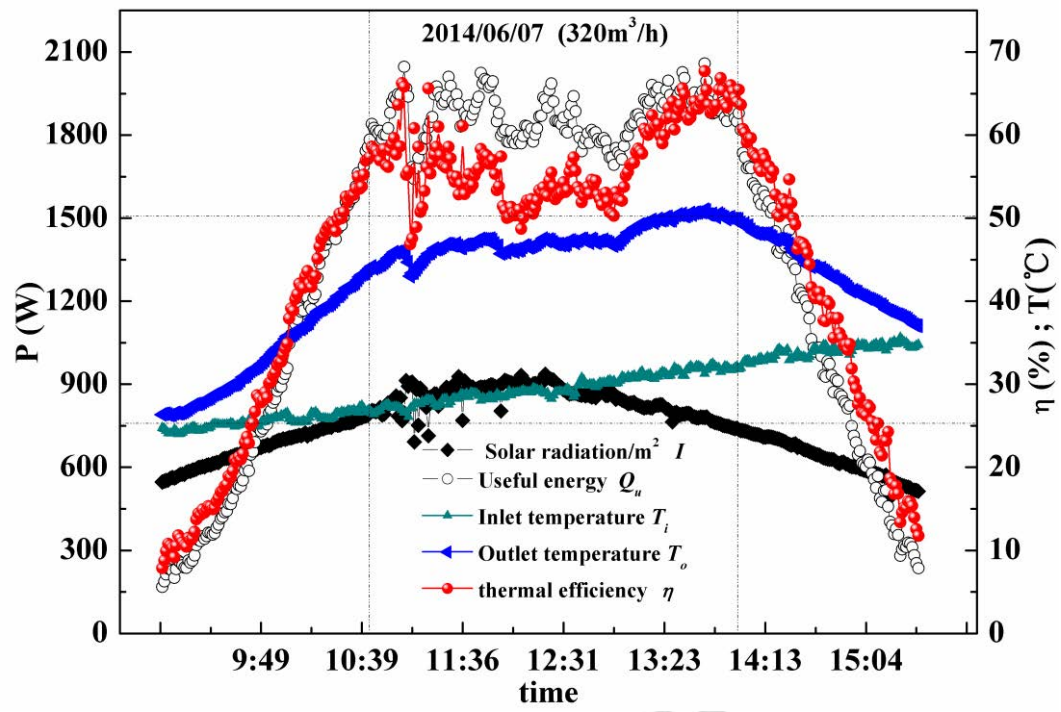

Fig. 13. Instantaneous thermal efficiency and solar radiation intensity versus time.

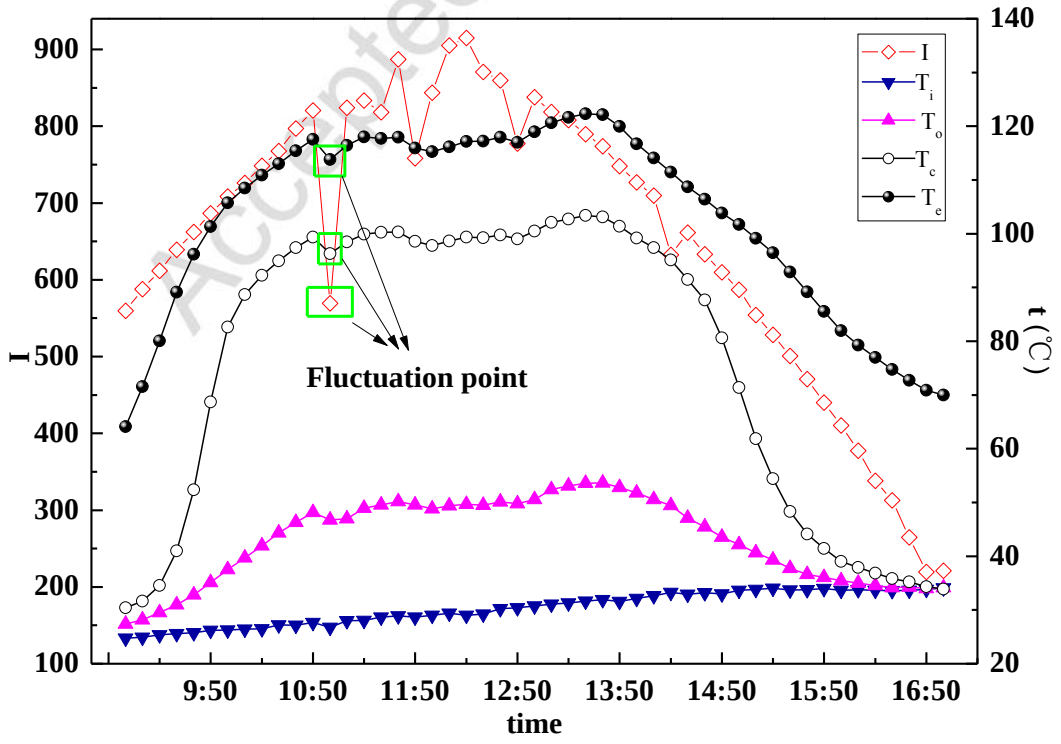

Fig. 14. Instantaneous temperature of the FMHPA and solar radiation intensity versus time.

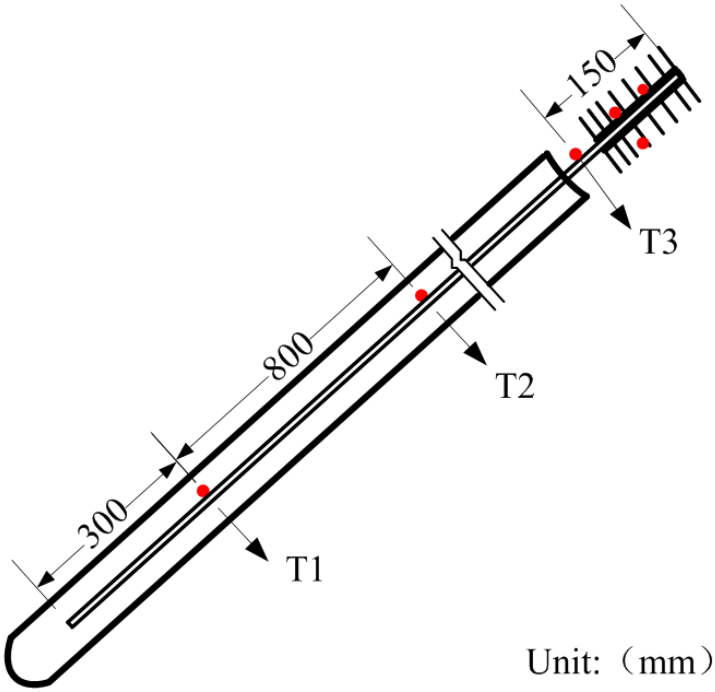

Fig. 15. Arrangement of thermocouples in the collecting unit.

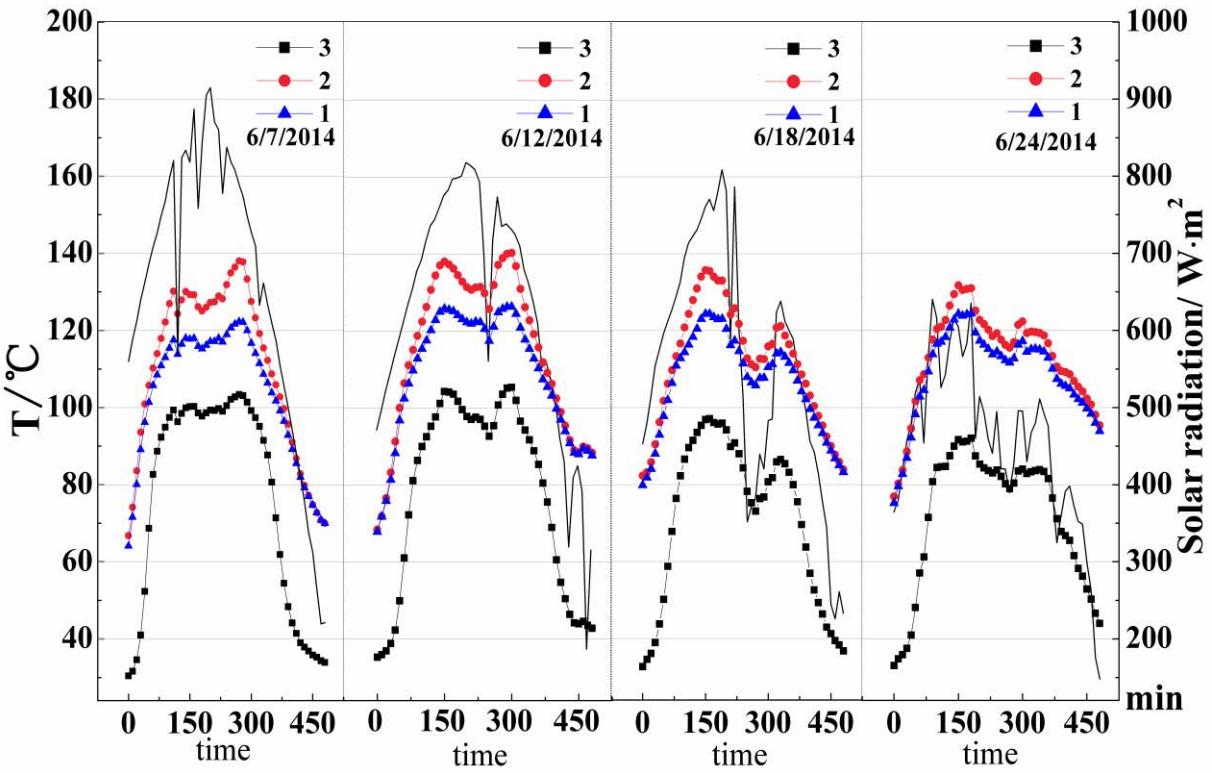

Fig. 16. Variation of temperature at different testing points on the FMHPA.

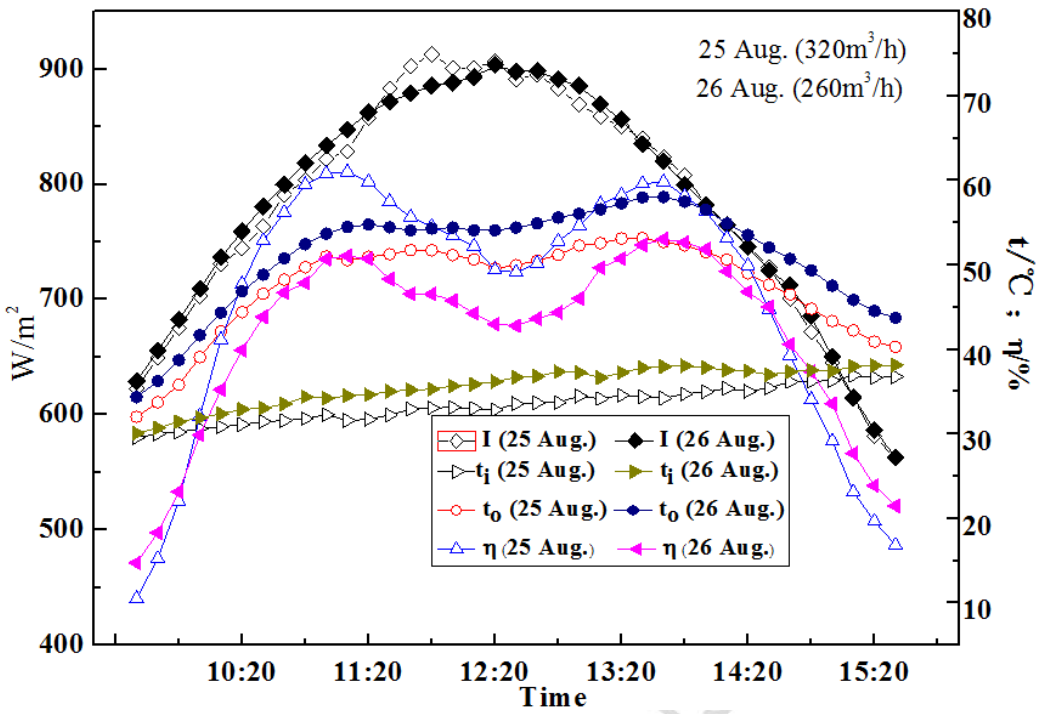

Fig. 17. Instantaneous thermal efficiency, solar radiation, inlet temperature, and outlet temperature versus time (time interval = 10 min).

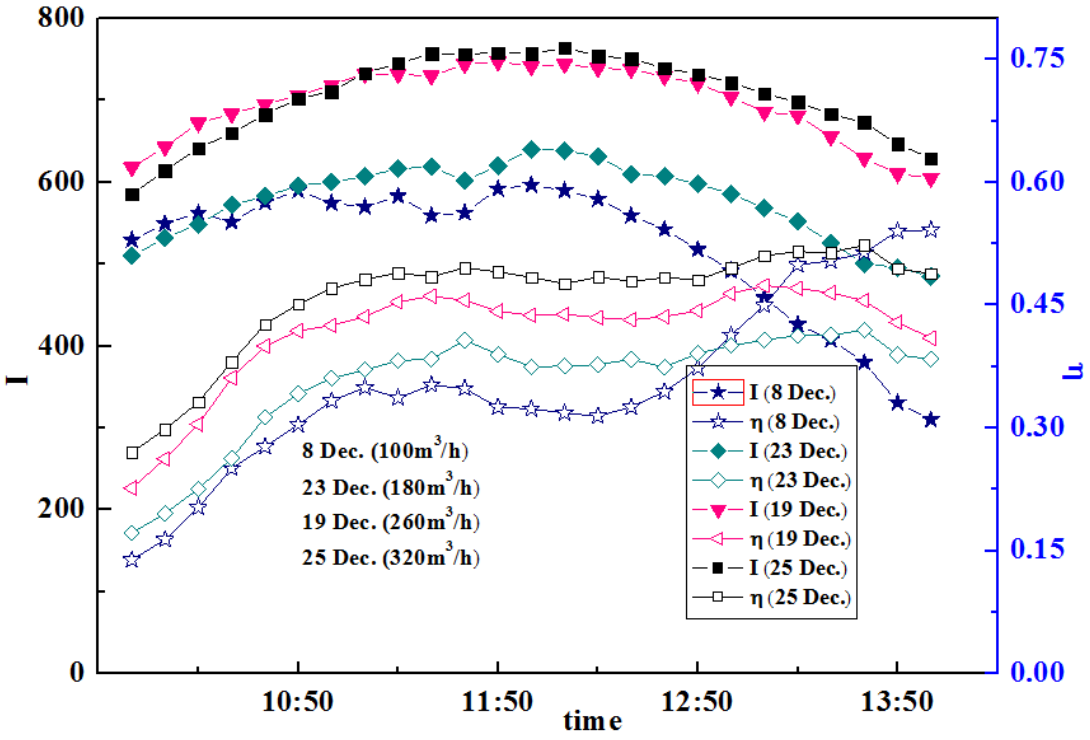

Fig. 18. Instantaneous thermal efficiency and solar radiation versus time.

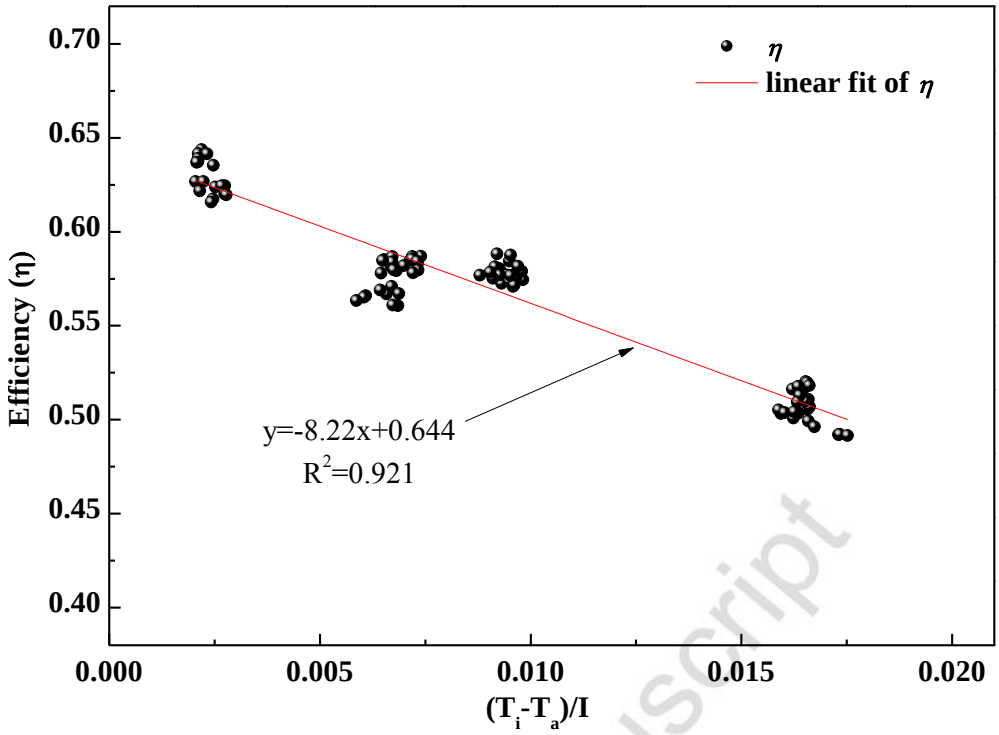

Fig. 19. Efficiency versus $(T_i - T_a)/I$.

Fig. 20. Schematic of the pressure drop test section.

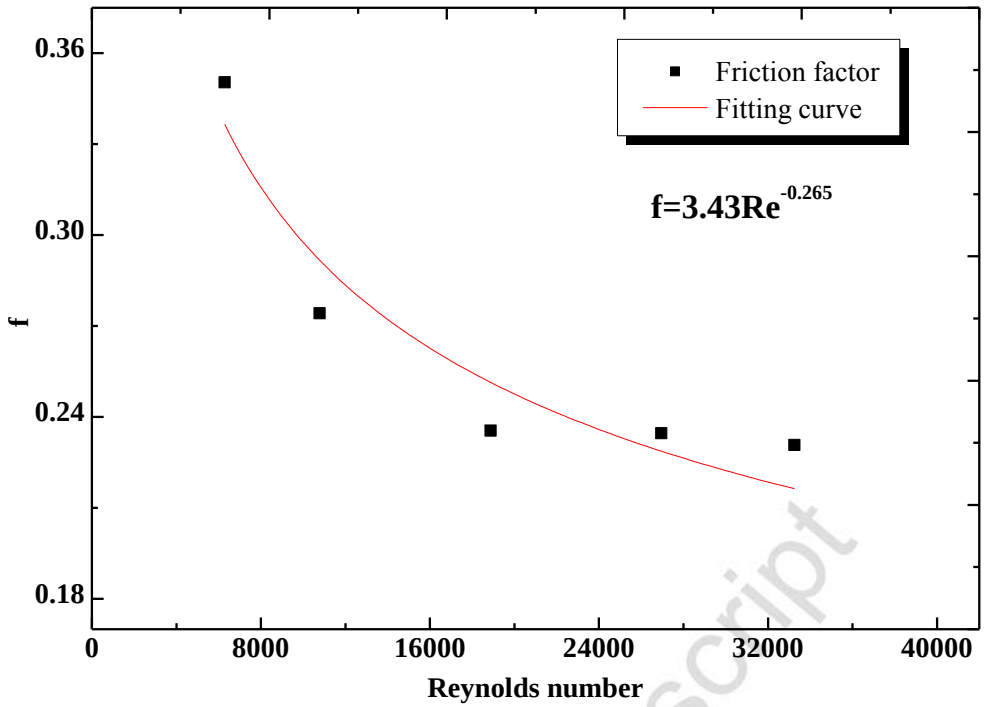

Fig. 21. Corresponding relationship between the Reynolds number and friction factor.

Table 1 Parameters of FMHPA-CPC SAC components.

Components	Specifications		
CPC	Width		268.4 mm
	Effective length		1,500 mm
	Height		186.5 mm
	Acceptance half angle of CPC		30°
	Reflectivity of CPC		92%
	CR		1.8
	Collector slope angle		45°
Vacuum glass tube	Diameter of cover glass tube		58 mm
	Diameter of inner glass tube		47 mm
	Length of glass tube		1,800 mm
	Coating film	Absorbance	95%
		Emittance	5%
		Transmittance	91%
	Borosilicate glass (3.3)	Heat conductivity coefficient	1.2 W/(m·K)
		Heat capacity	0.82 KJ/kg
Aluminum fins	82.5 × 144 × 27 mm	Fin height	27 mm
		Fin thickness	1 mm
		Fin spacing	6 mm
FMHPA	1,800 × 40 × 3 mm	Working fluid	Acetone
		Liquid filling ratio	20%
XPS	1. Thickness = 25 mm	Density	35 kg/m^3 to 40 kg/m^3
	2. Thickness = 50 mm	Thermal conductivity	0.03 W/(m·K)

Table 2 Information and uncertainties about the test instruments.

Device name	Model	Accuracy	Uncertainty values
Induced draft fan	TSKN0150	–	–
Data acquisition instrument	Agilent 34970A	–	–
Global radiation meter	TRT-2	<2%	0.50%
Thermocouple	WRNK-191	I	0.42%
Thermoresistance	Pt100WZPK-293	A, 0.15 °C	0.25%
Air volume cover	TSI8371	± 5%	2.66%
Differential manometer	Testo512	5%	4.00%
Anemovane	WS-8SX	Speed = ±0.3 m/s	3.00%
		Direction = ±3°	0.83%

Table 3 Parameters of the reflector.

Parameter	Value	Parameter	Value
τ	0.9	ρ_m	0.83
α	0.93	n	1.126
ρ	0.03	ρ^n	0.811
g	10 mm	p	0.932
r_1	23.5 mm	f_{ref}	1.0017
CR	1.8	ρ_r	0.07

Table 4 Experimental results of typical days in June (10:00 AM to 2:00 PM)

Date	Average solar radiation	Average inlet temperature	Average outlet temperature	Average temperature difference	Average efficiency
2014	W/m^2	°C	°C	°C	%
320 m^3/h					
7 June	799	28.85	45.89	17.04	61
12 June	744	36.02	49.36	13.34	50
18 June	615	31.00	41.73	10.73	48
24 June	513	31.86	39.65	7.79	46
260 m^3/h					
5 June	697	33.65	44.58	10.93	43
9 June	744	30.09	43.93	13.84	45
23 June	754	31.99	45.23	13.24	44